processes

MDPI

Article

Simulation and Multi-Objective Optimization of Three-Column Double-Effect Methanol Distillation by NSGA-III Algorithm

Weiye Chen, Zehua Hu, Xuechao Gao and Yefei Liu *

Research Center of Chemical Process Design, College of Chemical Engineering, Nanjing Tech University, Nanjing 211816, China

* Correspondence: yefei.liu@njtech.edu.cn

Abstract: The multi-objective optimization of methanol distillation is a critical and complex issue in the methanol industry. The three-column methanol distillation scheme is first simulated with Aspen Plus to provide the initial value of the NSGA-III algorithm. The operating parameters are optimized through the Python-Aspen platform. The total annual cost and CO_2 emissions are considered the objective function. A small value of indicator generational distance can be achieved by increasing the number of generations, which is helpful in improving algorithm convergence. The NSGA-III algorithm has good convergence and distribution performance. By comparing the optimized results with the original ones, the total annual cost and CO_2 emissions are, respectively, reduced by 5.35% and 12.80% when the operating parameters of the methanol distillation sequence are optimized through NSGA-III. As a result, substantial economic and energy savings can be made, offering great potential to improve the performance of the three-column methanol distillation.

Keywords: methanol; distillation sequence; NSGA-III; multi-objective optimization; process simulation

Citation: Chen, W.; Hu, Z.; Gao, X.; Liu, Y. Simulation and Multi-Objective Optimization of Three-Column Double-Effect Methanol Distillation by NSGA-III Algorithm. *Processes* **2023**, *11*, 1515. https://doi.org/10.3390/pr11051515

Academic Editors: Huairong Zhou, Dongliang Wang and Yong Yang

Received: 21 March 2023
Revised: 24 April 2023
Accepted: 25 April 2023
Published: 16 May 2023

1. Introduction

Methanol has wide industrial applications for the production of methylamine, formaldehyde, acetic acid, dimethyl ether, and methyl tert-butyl ether. In the methanol industry, crude methanol products are refined by distillation operations, which has a direct impact on the output and quality of methanol products [1]. Approximately 20% of the energy consumption in methanol production originates from the distillation units [2]. To save energy cost, some researchers developed extractive distillation for the production of ethanol [3–6]. To identify the minimum total annual cost, the optimization of distillation sequences was carried out for separating acetonitrile–methanol–benzene mixture [7]. However, the multi-objective optimization of methanol distillation sequences is still a much more essential task for the methanol industry.

Initially, the two-column methanol distillation scheme was commonly adopted to remove water and organic contaminants from crude methanol. At present, the three-column double-effect distillation scheme is widely applied due to its better performance. In this scheme, the methanol refining is separated into a pressurized column and an atmospheric column. The liquid from the bottom of the atmospheric column is heated by the gas from the top of the pressurized column. The three-column scheme has resulted in a significant decrease in energy consumption compared to earlier designs. For the three-column methanol distillation schemes, Xue et al. [8] developed a novel technology for three-column triple-effect methanol distillation, and the results revealed that the energy consumption was decreased by 20.91% compared to the three-column double-effect distillation scheme. However, they did not carry out the multi-objective optimization. The optimization of the operating parameters is non-trivial and needs some sophisticated mathematical algorithms rather than empirical attempts.

In recent years, the introduction of differential evolution algorithms has been favored to synchronously optimize chemical processes. Errico et al. [9] proposed a multi-objective

design approach for the optimization of distillation sequence systems. By combining this method with the differential evolution algorithm, the calculation time was reduced by 28% compared with the optimization, using only the differential evolution algorithm. Contreras-Zarazúa et al. [10] intensified the production process of diphenyl carbonate by the optimization involving cost and operating properties. The optimal configuration design of different reactive distillation towers was carried out. They found that the larger the liquid holding capacity and diameter of the tray, the better the control performance. Alcocer-García et al. [11] used differential evolution with tabu list as the optimization algorithm for optimizing the Eco-indicator 99 and the total annual cost of four different levulinic acid distillation sequences. Compared with the conventional scheme, both the Eco-indicator 99 and the total annual cost were reduced by the multi-objective optimization. However, compared with the genetic algorithm (GA), which is rich in individual selection strategies, the evolutionary mechanism of the differential evolution algorithm adopts a simple selection strategy, and it has not been optimized in advance for the parent individuals who participate in the reproduction, resulting in a low calculation efficiency.

At present, genetic algorithms have been widely used in many chemical process optimizations. The genetic algorithm is a search technique based on the principles of genetics and natural selection [12]. Since the conventional genetic algorithm chooses the best solutions based on random changes generated by the mutation operator, it is not guaranteed to find the optimal global solution to specific problems, but it is excellent at finding good, acceptable Pareto solutions [13]. With the continuous optimization of coding and convergence, the performance of the genetic algorithms is improved. Among them, the elite non-dominated sorted genetic algorithm-II (NSGA-II) can find the optimal solution approach to the Pareto front infinitely, and the crowding distance mechanism ensures that the optimal solution set has a good distribution. Tarafder et al. [12] presented a multi-objective optimization of the industrial ethylene reactor based on the elite non-dominated sorting genetic algorithm-II and finally obtained better operating parameters for the reactor. Although NSGA-II is widely applied because of its superior global search capability, its search accuracy is relatively poor, and the diversity remains to be enhanced because of blind spots.

The non-dominated sorting genetic algorithm (NSGA-III) based on the reference point was proposed by Deb and Jain [14]. It can balance the relationship between the accuracy of the optimization model and calculation time and effectively select the optimal point of the Pareto solution set, thus making the algorithm capable of dealing with multi-dimensional complex optimization problems efficiently. Pan et al. [15] proposed a multi-objective optimization for the separation of ethylbenzene from C8 aromatic hydrocarbons with extractive distillation, and the total annual cost and CO_2 emissions were minimized by NSGA-III to increase the economic and environmental benefits. Compared to conventional genetic algorithms, NSGA-III has a unique selection mechanism of non-dominated sorting based on the calculation distance of reference points [16], so it is necessary to apply NSGA-III for the multi-objective optimization of the methanol three-column distillation process.

If the operating cost for saving energy during methanol distillation is reduced excessively, equipment investments will increase. The present study aims at achieving optimal global results for the reduction in CO_2 emission and total annual cost of the process of three-column methanol distillation. Firstly, the three-column double-effect methanol distillation is designed, and the initial parameters of the process are determined by process simulation. Then, NSGA-III is used for the multi-objective optimization of the total annual cost and CO_2 emissions of the process, because the sequential optimization cannot comprehensively consider energy consumption and equipment investments. All of the algorithm parameters of the conventional genetic algorithm are empirical. In addition, differing from the optimization of genetic algorithm parameters used by Pan et al. [15], the effects of different algorithm parameters on the optimization results of methanol distillation are investigated in this work to determine the appropriate algorithm parameters. In addition, the evaluation indicators and the minimum Euclidean distance are determined to find the optimal point

in the Pareto front. Finally, the multi-objective optimization of three-column methanol distillation is achieved. The optimal global solution can be obtained through the above explorations of different algorithm parameters and evaluation indicators.

This work is organized as follows. The process simulation of the methanol distillation unit is shown in Section 2. In Section 3, the process parameters optimization through NSGA-III is reported for the three-column double-effect methanol distillation. Performance indexes of total annual cost (TAC) and CO_2 emissions are considered as the objective function. Pareto optimal solutions set and other evaluation indexes, which are presented to satisfy the multi-objective optimization for process design and operation, are obtained and reported in Section 4. The conclusions are given in Section 5.

2. Process Simulation

2.1. Implementation of The Base Simulation Model

Before building the multi-objective optimization model, the process simulation with Aspen Plus v11 was carried out to provide the initial values for the optimization procedure. It is worth noting that recent methods have been proposed to overcome the burden linked to simulation costs using analytical simplifications, and "analytical Real Time Optimization" is a typical example based on an offline simulation model [17]. The thermodynamic model NRTL-RK is selected to predict the interaction among the components since NRTL can predict the equilibrium for polar mixtures and calculate the activity coefficients in the liquid phase of each column properly. The RK state equation can also predict nonpolar compounds in the vapor phase. According to industrial uses, the purity of the refined methanol is set at 99.9 wt%, and the methanol content of the wastewater at the bottom of the atmospheric column is required to be less than 0.3 wt%. The composition of the crude methanol feed is presented in Table A1 in the Appendix A section. The temperature, pressure, and mass flow rate of the feed are 40 °C, 5000 kPa, and 169,068.75 kg/h, respectively.

With the three-column arrangement, shown in Figure 1, the crude methanol is purified via pre-run column T1, higher pressure column T2, and atmospheric column T3. To reduce energy consumption, the overhead vapor of the high-pressure column T2 heats the sum of the atmospheric column T3. After removing part of the soluble gas by expansion tank, the crude methanol enters T1 near the top stage. T1 operates at a pressure slightly higher than atmospheric pressure. The methanol vapor generated in the reboiler of T1 acts to strip the light ends (such as dimethyl ether, hydrogen, and nitrogen) and residual dissolved gas from the crude methanol. The bottom product of T1 is pressurized and then sent to T2, operating at a pressure of 0.81–0.86 MPa, where approximately 50% of methanol can be produced as the overhead product. Then, the bottom product of T2 flows into T3. In T3, the remaining methanol is obtained as the overhead product, while wastewater is withdrawn as the bottom product. The middle boiling impurities (mainly *n*-butanol) are withdrawn as a side stream below the feed stage.

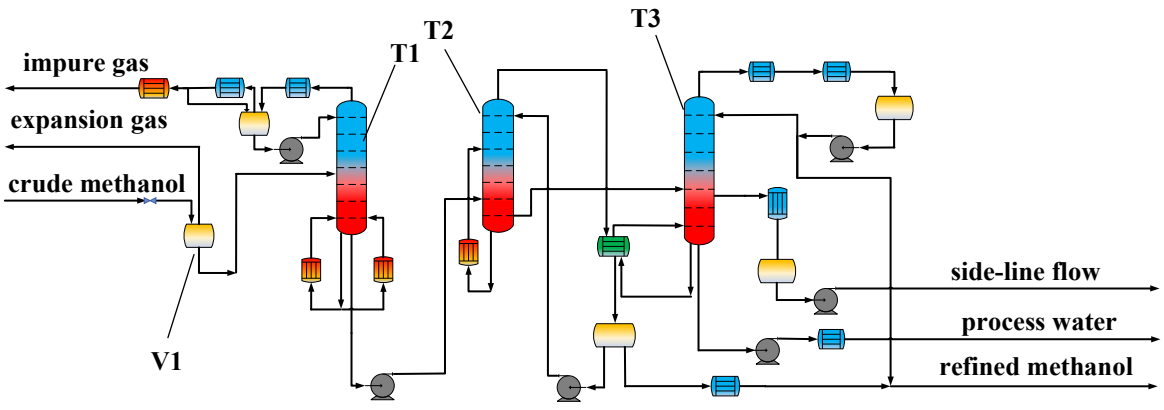

Figure 1. Schematic of the three-column double-effect methanol distillation scheme. (V1: expansion tank; T1: pre-run column; T2: high-pressure column; and T3: atmospheric column).

2.2. Data Reconciliation

This method was proposed by Vaccari et al. [18]. The optimization variables used for reconciling the available data, are the following:

- RR_1: the mole reflux ratio of T1
- RR_2: the mole reflux ratio of T2
- RR_3: the mole reflux ratio of T3

The objective function φ used for the data reconciliation procedure is based on the errors between measured ($\overline{\phi_i}$) and predicted model (ϕ_i) values of selected key quantities. The quantities taken into consideration are the top temperature of the three columns, the bottom temperature of the three columns, and the mass flow rate of the refined methanol, process water, side stream. The various terms of the objective function have all been normalized in the following way:

$$\varphi = \sum_{i=1}^{6} \left| \frac{\phi_i - \overline{\phi_i}}{\overline{\phi_i}} \right| \quad (1)$$

Different runs of the following optimization problem have been executed to find the optimal combination of variables values:

$$\min_k \varphi(k) \quad (2)$$

Subject to

$$k_{\min} \leq k \leq k_{\max} \quad (3)$$

in which $k = [RR_1; RR_2; RR_3]$, $k_{\min} = [0.01; 0.01; 0.01]$, and $k_{\max} = [5; 5; 5]$. The optimization problem is solved using the sensitivity analysis tool in Aspen Plus v11, and the optimal values are reported in Table 1.

Table 1. Optimal values obtained with data reconciliation of methanol distillation.

Quantity	Initial Values	Optimal Values
RR_1	1.053	0.085
RR_2	0.715	1.169
RR_3	0.732	0.605

To obtain the calibration values of the operating parameters, the design specifications are carried out in the rigorous simulation of the three-column double-effect methanol distillation without separating the reboilers and condensers from the columns. The calibration values are close to the data from the actual process. After data reconciliation, the comparison results are shown in Table 2. Except for the side stream flow rate, the relative error between simulation values and calibration values is within the acceptable range, indicating that the simulation results are accurate. The process simulation results from Aspen Plus can be used for the subsequent optimization of the distillation sequence.

Table 2. Comparison results between simulation values and calibration values.

Operating Parameters	Calibration Values	Simulation	Relative Error
T1 top/bottom temperature (°C)	82/90	82.7/90.1	0.85%/0.11%
T2 top/bottom temperature (°C)	127.2/135	128.7/134.4	1.18%/0.44%
T3 top/bottom temperature (°C)	41/116	41/116.8	0.00%/0.69%
Refined methanol flow rate (t/h)	149.591	149.592	0.00067%
Process water flow rate (t/h)	12.600	12.472	1.02%
Side stream flow rate (t/h)	1.250	1.359	8.72%

3. Optimization of Distillation Sequence

3.1. NSGA-III

The basic process of NSGA-III is similar to that of the genetic algorithm, and it adds a fast non-dominated sorting operation from NSGA-II and introduces reference lines for the non-dominance ranking of individuals, effectively reducing the range of multi-dimensional search space, and making the search process clearer. The NSGA-III algorithm is shown in Figure 2.

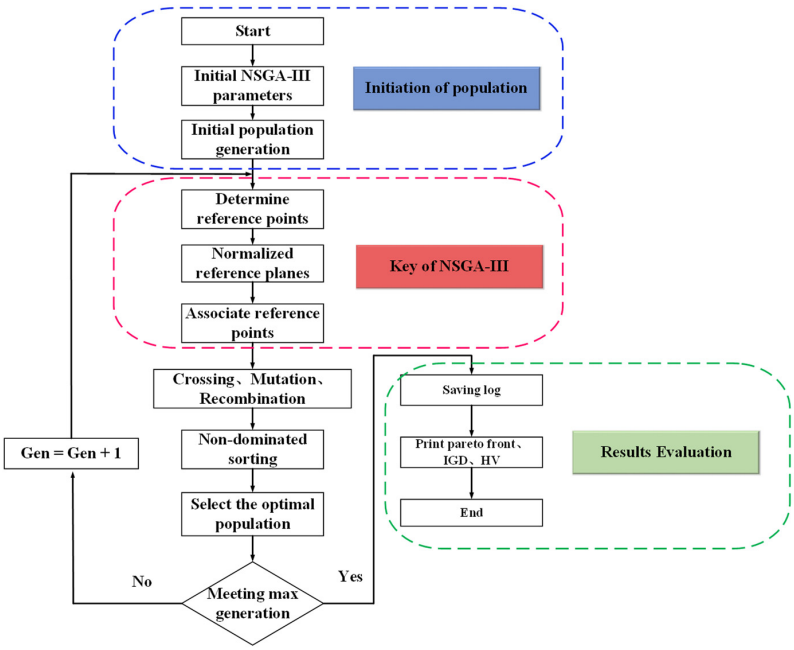

Figure 2. NSGA-III algorithm.

Figure 3 shows the distribution of 3D elevation reference points [19]. NSGA-III selects the reference points from the bottom and the number of reference points becomes fewer. The vector is constructed from the reference point to the origin, and the distances to the reference point for each population individual are calculated. Finally, the nearest reference point and the shortest distance are determined.

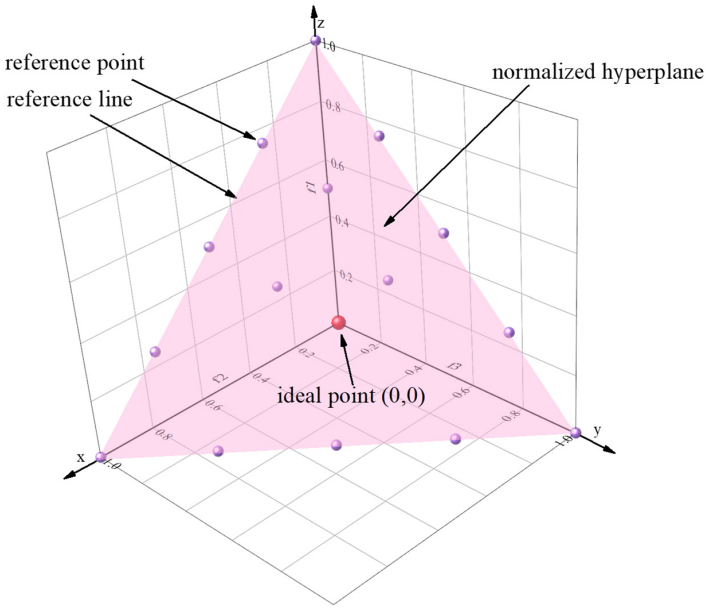

Figure 3. The distribution of 3D elevation reference points.

The implementation of this optimization method is conducted through a hybrid platform using Python v3.9 and Aspen Plus v11. The vectors of decision variables are sent from Python to Aspen Plus through COM technology [20]. In Python, the vectors are attributed to the process variables that will be evaluated by Aspen Plus. After the simulation is finished, Aspen Plus returns the vector to Python. Then, the optimization model is solved based on the NSGA-III algorithm toolbox "Geatpy" in Python. Finally, the process is repeated until the maximum generation is reached, and the values of the objective functions are obtained. The procedure of the optimization with the NSGA-III is shown in Figure 4.

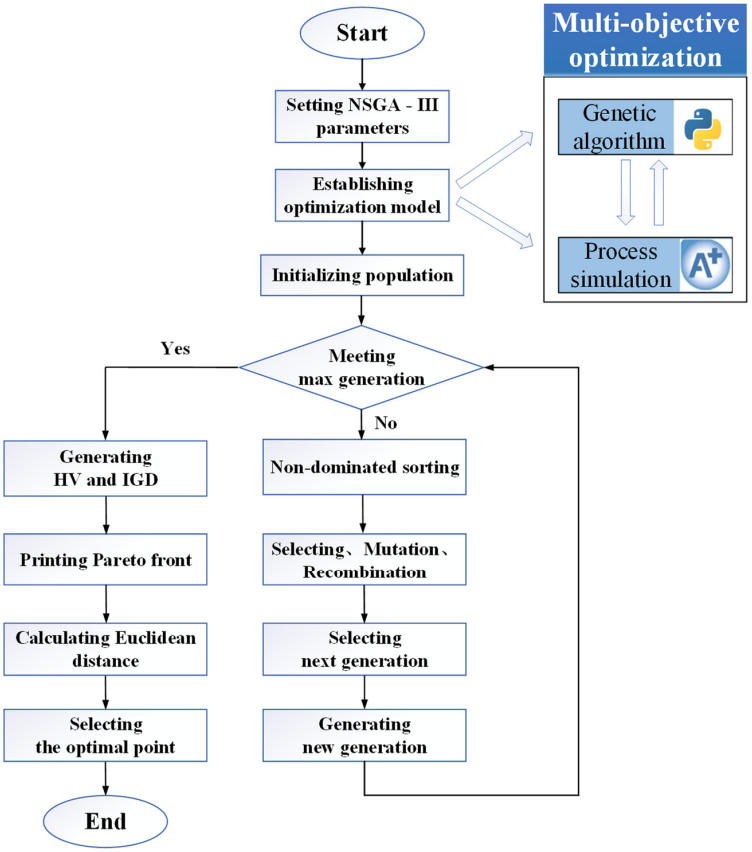

Figure 4. The flowsheet of the NSGA-III procedure.

3.2. Performance Parameters

3.2.1. Population Size

Population size directly affects the calculation time and population diversity. If the value of population size is too large, the optimal solution set in the Pareto front curve will be uniformly distributed, but the calculation time is long. Otherwise, the algorithm has low complexity and converges prematurely, resulting in the non-uniform distribution of Pareto solution sets. It is necessary to explore the suitable population size for the optimization model.

The total annual cost (TAC) is selected as the assessment indicator. With the population size P, the optimal values x_i of n non-dominant individuals obtained after running the NSGA-III program. Solution accuracy S is defined in Equation (4):

$$S = \frac{x}{x_0} \tag{4}$$

where x_0 is the global optimal solution, x is the local optimal solution and the minimum value of TAC. After the program runs terminally, the global optimal solution x_0 can be

obtained by calculating the minimum Euclidean distance in the Pareto dataset, and the local optimal solution x is the minimum value of TAC in the Pareto dataset.

Figure 5a presents the relationship between the population size and the total annual cost. It is seen that the local optimal solution x is smaller than the global optimal solution x_0, so all values of S range between (0 and 1). To determine the suitable population size, the curve fitting following Equation (5) is made by taking P as the independent variable and S as the dependent variable. The fitting parameters are listed in Table 3. The good fitting curve is shown in Figure 5b. It is observed that S increases with P. However, S has a slight decrease when P is larger than 110. As a result, this study chooses 110 as the suitable value of P.

$$f(x) = a\exp(bx) + c\exp(dx) \tag{5}$$

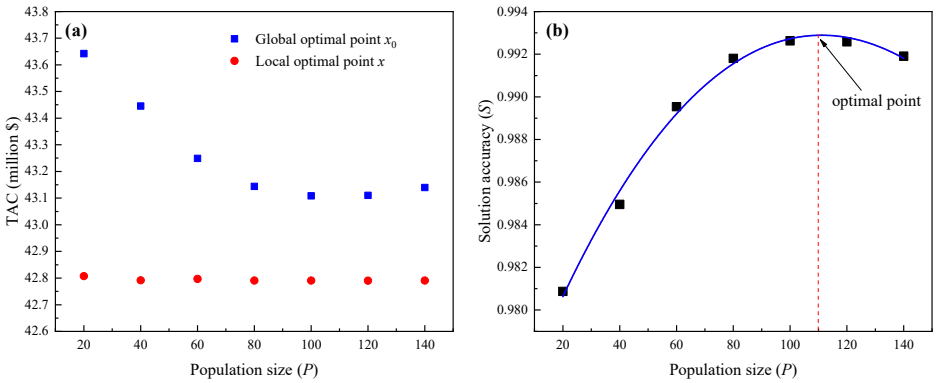

Figure 5. (**a**) Relationship between population size P and total annual cost; and (**b**) Curve fitting between population size P and solution accuracy S.

Table 3. Parameters of fitting results.

Parameter Values				
a	***B***	***c***	***d***	R^2
78.34715	−0.00163	−77.37291	−0.00165	0.98875

3.2.2. Objective Function

To achieve the two goals of cost saving and emission reduction, two objective functions are defined as follows:

$$f_1(x) = \min[f_1(N_{Ti}, N_{Fi})]\ i = 1, 2, 3 \tag{6}$$

$$f_2(x) = \min[f_2(N_{Ti}, N_{Fi})]\ i = 1, 2, 3 \tag{7}$$

where $f_1(x)$ is the global minimum of total annual cost (million$); $f_2(x)$ is the global minimum of CO_2 emissions (kt/year); N_{Ti} is the total number of the ith column trays; and N_{Fi} is the feed plate of the ith column.

TAC is calculated as follows [21,22]:

$$\text{TAC} = C_E + \frac{C_C}{P_{payback}} \tag{8}$$

where C_E is the annual operating cost, including low-pressure steam and condensate (million$); C_C is the equipment investments, including heat exchanger cost, pump cost, and column vessel cost (million$); and $P_{payback}$ is the payback period (3 years).

The annual operating cost is calculated as

$$C_E = 8000(31.432m_{LS} + 0.1525m_{cw} + 0.118E) \tag{9}$$

where M_{LS} is the annual consumption of low-pressure steam (t/year, 1 MPa); M_{CW} is the annual consumption of cooling water (t/year, 20 °C); and E is the annual power consumption (kW·h/year).

The equipment cost C_C is calculated as

$$C_C = C_V + C_{HE} + C_P \tag{10}$$

where the pump cost C_P is calculated as 0.01 million$.

The column cost C_V is calculated as

$$C_V = 17640D^{1.066}(0.7315N)^{0.802} \tag{11}$$

where D is column diameter (m) and N is the total number of trays.

The heat exchanger cost C_{HE} is calculated as

$$C_{HE} = 7296A^{0.65} \tag{12}$$

where A is the heat exchang area (m^2).

By considering the impact of distillation separation on the environment, the indicator of environmental performance is CO_2 emissions. The CO_2 emissions mainly come from the reboilers at the bottom of the columns. This methodology was proposed by Gadalla et al. [23], and CO_2 emissions can be calculated as

$$[CO_2]_{\text{emissions}} = \alpha\left(\frac{Q_{Fuel}}{NHV}\right)\left(\frac{C\%}{100}\right) \tag{13}$$

where Q_{fuel} is amount of fuel burnt (kW); α is the ratio of molar masses of CO_2 and C; and NHV represents the net heating value of fuel with a carbon content of C% (kJ/kg).

The present study uses a NumPy array matrix in Geatpy to store the objective function value of the population. It is named ObjV. Each row corresponds to each individual, and each column corresponds to an objective function. Therefore, ObjV in this study is a binary function matrix, which is expressed as follows:

$$\text{ObjV}\begin{pmatrix} f_1(x_{1,1}, x_{1,2} \ldots x_{1,6}) & f_2(x_{1,1}, x_{1,2} \ldots x_{1,6}) \\ f_1(x_{2,1}, x_{2,2} \ldots x_{2,6}) & f_2(x_{2,1}, x_{2,2} \ldots x_{2,6}) \\ \vdots & \vdots \\ f_1(x_{n,1}, x_{n,2} \ldots x_{n,6}) & f_2(x_{n,1}, x_{n,2} \ldots x_{n,6}) \end{pmatrix} \tag{14}$$

3.2.3. Constraint Function

Before the optimization of the distillation sequence, the purity of the corresponding substances in the discharge stream must be qualified, and the recovery rate of the key components must meet the requirements. In order to ensure that the flow rate and purity of methanol at the top of T2 and T3 meet the requirements, the design specifications of the distillation columns are used to set the recovery rate of the key components at the top and bottom of each column, which ensures that the reflux ratio and the flow rate of the column bottom are the output results. The constraint functions are defined as follows:

$$\text{CVV} = \begin{pmatrix} c_{1,1} & c_{1,2} & \cdots & c_{1,6} \\ c_{2,1} & c_{2,2} & \cdots & c_{2,6} \\ \vdots & \vdots & \vdots & \vdots \\ c_{n,1} & c_{n,2} & \cdots & c_{n,6} \end{pmatrix} \tag{15}$$

where in the matrix, column 1 represents the reflux ratio of T1, column 2 represents the flow rate of the T1 bottom, column 3 represents the reflux ratio of T2, column 4 represents the

flow rate of T2 bottom, column 5 represents the reflux ratio of T3, and column 6 represents the flow rate of T3 bottom, respectively.

The NumPy array matrix CVV (Constraint Violation Value) in Geatpy is used to store the degree of violation of each constraint condition by population individuals. If an element of the CVV matrix is less than or equal to 0, it means that the corresponding individual element satisfies constraint conditions. Otherwise, it means the constraint is violated. The reflux ratios and bottom flow rates of three columns are filled into the CVV matrix by taking the opposite numbers of these six parameters. Then, the communication between python and Aspen Plus can be operated in a dynamic fashion well.

3.2.4. Decision Variables

Under the condition that the pressure of the three columns and the constraint conditions are defined, there are six key operating variables that can be adjusted in this study, which are the total number of trays of the three columns and the corresponding feed plate.

Considering that if the feed plate position is directly specified, the index number of the feed plate may be greater than the total number of trays, causing the process of sending parameters into Aspen Plus to terminate. Hence, the feed plate is changed to the ratio of the feed plate to the total number of trays in this study, and the results are rounded down to ensure that the index number of the feed plate is always smaller than the total number of trays. To ensure that the mass purity of the product reached 99.9%, the design specifications are set in the RadFrac block. At the same time, the molar recoveries of the key components are specified as 99.9%. The six operating variables are chosen as decision variables, which are given in Table 4.

Table 4. Range of decision variables.

Decision Variables	Range
Total number of T1 trays	[30, 60]
The ratio of the index number of feed plate to total number of T1 trays	[0.20, 0.48]
Total number of T2 trays	[65, 100]
The ratio of the index number of feed plate to total number of T2trays	[0.7, 0.95]
Total number of T3 trays	[65, 100]
The ratio of the index number of feed plate to total number of T3 trays	[0.53, 0.95]

4. Optimization Results and Discussion

The optimization procedure is carried out on a 64-bit desktop computer with an Intel Core i7-8700 CPU @3.20 GHz, including 32 GB RAM. The results of indicator generational distance, hypervolume, and Pareto optimal solutions are discussed.

4.1. Indicator Generational Distance

The indicator generational distance (IGD) [24], one of the indexes of evaluating the effectiveness of evolutionary algorithms, indicates the average distance from individuals in the Pareto front to the non-dominated solution found by the evolutionary algorithm, which means that the smaller the value of IGD, the better the performance of the algorithm. Its definition is as follows:

$$\mathrm{IGD} = \frac{\sum_{v \in P} d(v, Q)}{|U|} \tag{16}$$

where U is the point set uniformly distributed on the real Pareto surface, $|U|$ is the number of individuals, Q is the optimal Pareto solution set, and d (v, Q) is the minimum Euclidean distance from individual v to population.

The IGD results of the population evolution process under different generations are shown in Figure 6. With the increase in evolution generations, IGD value decreases sharply and tends to be stable, which indicates that the optimization algorithm has good convergence. In the late evolution period, the local optimal solution of the individual

population tends to be the global optimal solution. In addition, when IGD tends to be stable, the larger number of generations leads to a smaller value of IGD, indicating that increasing number of generations is helpful to further improve the convergence of the algorithm.

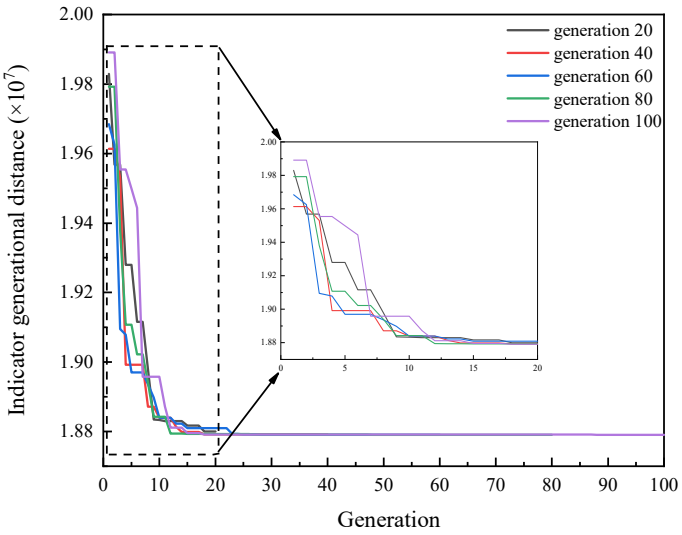

Figure 6. The IGD results under different generations.

4.2. Hypervolume

The hypervolume (HV) evaluation method was first proposed by Zitzler [25]. It represents the volume of the hypercube enclosed by the non-dominated solution set and reference points in the target space obtained by the multi-objective optimization algorithm, which means that the bigger the value of HV, the better the performance of the algorithm. HV is defined as follows:

$$\mathrm{HV} = \delta\left(\bigcup_{i=1}^{|S|} v_i\right) \tag{17}$$

where δ is used to measure volume, $|S|$ is the number of non-dominated solution sets, and v_i is the super volume formed by the reference point and the i_{th} solution in the solution set.

Since the calculation accuracy of the hypervolume depends on the selection of reference points and the number of non-dominant individuals, the changing trajectory of HV is recorded with the increase in generations, which is shown in Figure 7. It can be seen that under different generations, HV values fluctuate greatly at the initial stage of evolution and tend to be stable at the later stage of evolution, indicating that the number of non-dominated individuals is increasing rapidly at the initial stage of evolution and the non-dominated solution set reaches saturation later, which further shows that the algorithm has good convergence and distribution performance. In addition, the reason why HV values tend to be larger under 60 and 40 generations is that both the numbers of non-dominant individuals are greater than those under other generations. The number of non-dominant individuals under different generations is shown in Table 5.

Table 5. The number of non-dominant individuals under different generations.

Generation	Non-Dominant Individuals
20	62
40	75
60	75
80	69
100	70

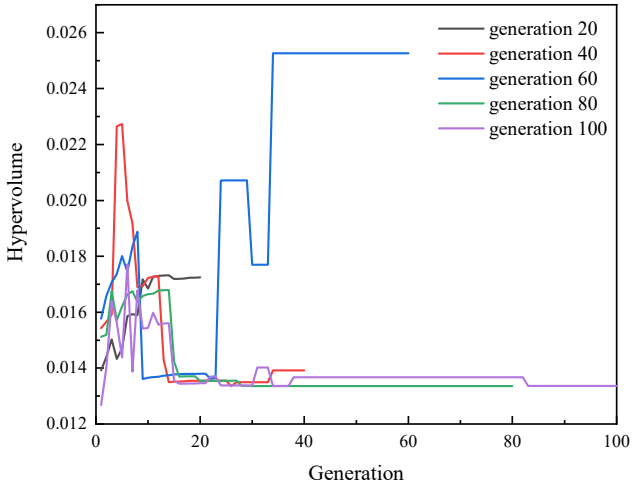

Figure 7. The HV tracking results under different generations.

4.3. Selection of The Optimal Point

Figure 8 shows all points on the Pareto front curve under different generations. These points are the optimal solution set by considering all weight combinations which are calculated based on NSGA-III. The evaluation of ideal optimization results depends on whether points are evenly distributed and continuous. It can be seen from the comparison that when the generation is 100, the Pareto front curve is evenly distributed and is very close to the real Pareto frontier, thus it is selected as the optimal solution set.

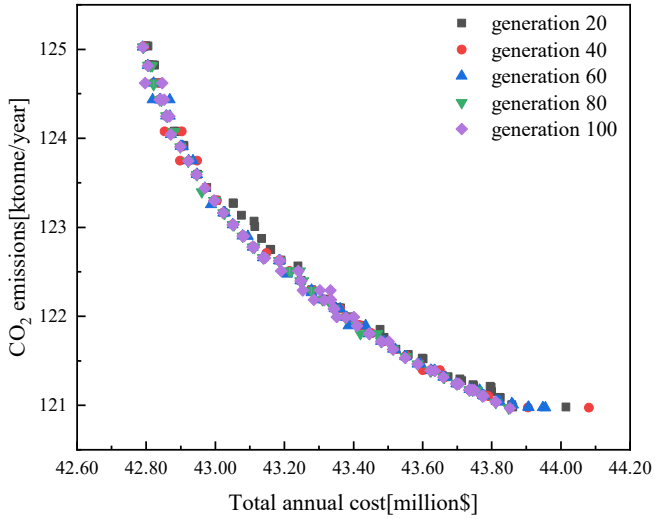

Figure 8. The Pareto front curve.

In industrial production, it is necessary to select one of the best points. In this study, the technique for order preference by similarity to an ideal solution (TOPSIS), proposed by Hwang and Yoon [26], is used to rank the evaluation object by detecting the distance between the optimal solution and the worst solution, and then the best point on the Pareto front can be selected.

The selection steps are as follows: Firstly, the total annual cost and CO_2 emissions are normalized, as shown in Figure 9. Then, the "ideal point" according to the optimization model is selected, which is (0,0), which meets the minimum annual total cost and CO_2 emissions in this study. Finally, the distance between the point on the Pareto front curve and the "ideal point" is calculated according to the Euclidean distance formula, and the minimal value point is selected as the optimal point on the Pareto front curve, as shown in Figure 10.

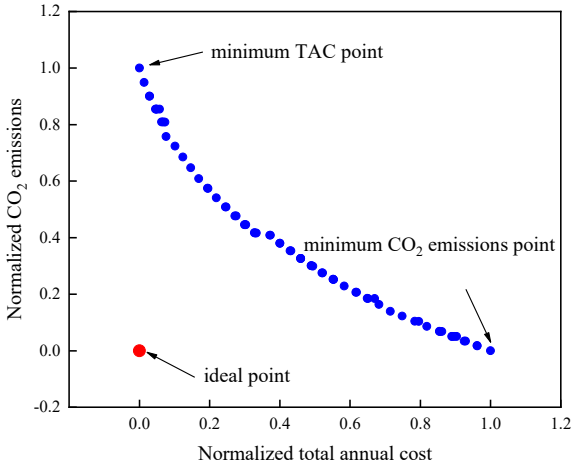

Figure 9. The normalized results of total annual cost and CO_2 emissions.

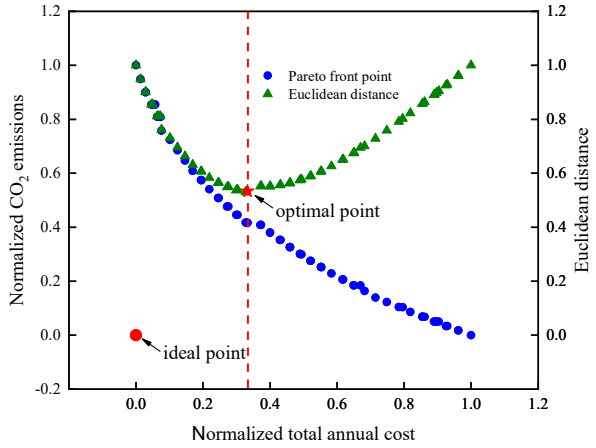

Figure 10. The Euclidean distance results.

Figure 11 gives the comparison between the original and optimized results of total annual cost and CO_2 emissions. By optimizing the operating parameters of the methanol distillation sequence through NSGA-III, the total annual cost and CO_2 emissions are, respectively, reduced by 5.35% and 12.80%, indicating that the optimization performance is favorable. The optimized results of each operating variable are shown in Table 6. The total annual cost and CO_2 emissions have both decreased. The tray number of column T1 decreased from 40 to 30, and the index number of feed plate decreased from 11 to 9. The tray number of column T2 decreased from 85 to 80, and the index number of feed plate remained the same. The tray number of column T3 decreased from 85 to 65, and the index number of feed plate decreased from 62 to 35. By optimizing the operating parameters of the distillation sequence through NSGA-III, the total annual cost is reduced by 2.44 million$, and CO_2 emissions are reduced by 18.01 kt/year. It can be concluded that compared with the operating cost, the equipment cost has a greater impact on the performance of the methanol distillation sequence, so it is necessary to use fewer trays to reduce the total annual cost.

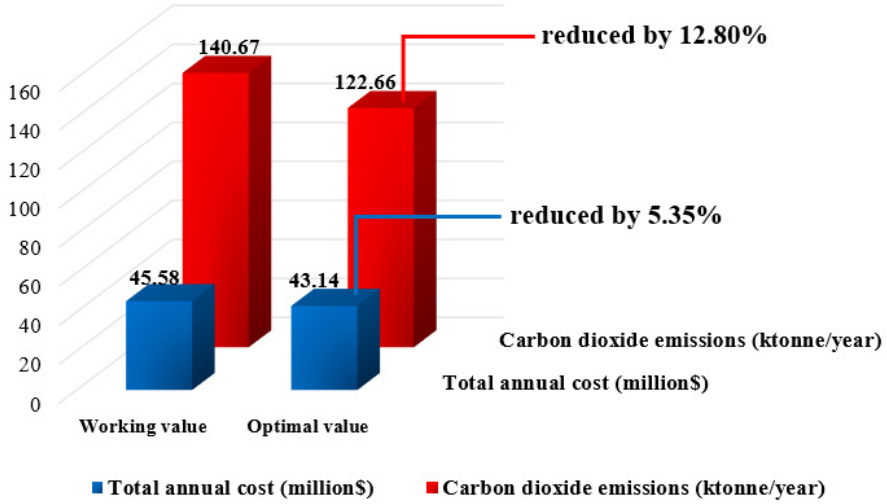

Figure 11. Comparison between the original and optimized results of total annual cost and CO_2 emissions.

Table 6. Multi-objective optimization results and optimal operating variables.

Operating Parameters	Plant Data	Optimal Values	Adjustment Strategy
Total number of T1 trays	40	30	↓
The index number of feed plate in T1	11	9	↓
Total number of T2 trays	85	80	↓
The index number of feed plate in T2	76	76	-
Total number of T3 trays	85	65	↓
The index number of feed plate in T3	62	35	↓
TAC (million$)	45.58	43.14	
CO_2 emissions (kt/year)	140.67	122.66	

5. Conclusions

The high energy consumption is the main issue of three-column methanol distillation. In order to achieve multi-objective optimization of three-column methanol distillation, a strategy is put in place: optimizing the operating parameters to simultaneously minimize the CO_2 emissions and total annual cost. The optimization method is based on the NSGA-III algorithm, which is implemented through a hybrid platform using Python v3.9 and Aspen Plus v11. The good convergence of NSGA-III was found by investigating the indicator generational distance and the hypervolume. The evaluation indicators and the minimum Euclidean distance were determined to find the optimal point in the Pareto front. The TOPSIS method is applied to search for the optimal point on the Pareto front curve, which explores an overall solution of distillation sequence design. Through multi-objective optimization, the total annual cost and CO_2 emissions are reduced by 5.35% and 12.80%, respectively, which guarantees low economic and environmental impacts. The total numbers of column T1 and T3 trays in the methanol distillation sequence are reduced due to the optimization, indicating that the equipment cost plays a key role in reducing the total annual cost. The NSGA-III algorithm provides a new way to optimize the methanol distillation system in the industry.

Author Contributions: Conceptualization, W.C. and Y.L.; methodology, W.C.; software, W.C. and Z.H.; validation, W.C. and Y.L.; formal analysis, W.C.; investigation, X.G.; resources, X.G.; data curation, Y.L.; writing—original draft preparation, W.C.; writing—review and editing, Y.L.; supervision, Y.L.; project administration, Y.L. and X.G.; funding acquisition, Y.L. and X.G. All authors have read and agreed to the published version of the manuscript.

Funding: This research was funded by the Natural Science Foundation of Jiangsu Province (BK20160978) and National Natural Science Foundation of China (22178166).

Institutional Review Board Statement: Not applicable.

Informed Consent Statement: Not applicable.

Data Availability Statement: Data are contained within the article.

Conflicts of Interest: The authors declare no conflict of interest.

Nomenclature

GA	Genetic algorithm
NSGA	Non-dominated sorting genetic algorithm
TAC	Total annual cost [million$]
T1	The pre-run column
T2	The high-pressure column
T3	The atmospheric column
RR_1	The mole reflux ratio of T1
RR_2	The mole reflux ratio of T2
RR_3	The mole reflux ratio of T3
$\overline{\phi_i}$	Measured values of selected key quantities
ϕ_i	Predicted model values of selected key quantities
k	The values of RR_1, RR_2, and RR_3
k_{min}	The minimum value of k
k_{max}	The maximum value of k
P	The population size
S	Solution accuracy
x_0	The global optimal solution
x	The local optimal solution
$f_1(x)$	The global minimum of total annual cost [million$]
$f_2(x)$	The global minimum of CO_2 emissions [kt/year]
N_{Ti}	The total number of the ith column trays
N_{Fi}	The feed plate of the ith column
C_E	The annual operating cost [million$]
C_C	The equipment investments [million$]
$P_{payback}$	The payback period
M_{LS}	The annual consumption of low-pressure steam [t/year, 1 MPa]
M_{CW}	The annual consumption of cooling water [t/year, 20 °C]
E	The annual power consumption [kW·h/year]
C_P	The pump cost [million$]
C_V	The column cost [million$]
D	The column diameter [m]
N	The total number of trays
C_{HE}	The heat exchanger cost [million$]
A	The heat exchanger area [m^2]
$[CO_2]_{emissions}$	The CO_2 emissions [kt/year]
Q_{fuel}	The amount of fuel burnt [kW]
α	The ratio of molar masses of CO_2 and C
NHV	The net heating value of fuel with carbon content of C% [kJ/kg]
ObjV	The matrix of storing the objective function value
CVV	The matrix of storing the constraint violation value
IGD	The indicator generational distance
U	The point set uniformly distributed on the real Pareto surface
$\|U\|$	The number of individuals
Q	The optimal Pareto solution set
$d(v, Q)$	The minimum Euclidean distance from individual v to population
HV	The hypervolume index

δ	The measurement of volume
$\|S\|$	The number of non-dominated solution sets
v_i	The super volume formed by the reference point
TOPSIS	The technique for order preference by similarity to an ideal solution

Appendix A

Table A1. Crude methanol feed data.

Component	Mass Fraction
carbon monoxide	0.0233
carbon dioxide	0.0002
hydrogen	0.0001
nitrogen	0.0019
methane	0.0001
methanol	0.8902
water	0.0767
dimethyl ether	0.0020
n-butanol	0.0046
acetone	0.0007
ethanol	0.0002

References

1. Sun, J.S.; Li, X.G. A hybrid design combining double-effect thermal integration and heat pump to the methanol distillation process for improving energy efficiency. *Chem. Eng. Process.* **2017**, *119*, 81–92.
2. Tijm, P.J.A.; Waller, F.J.; Brown, D.M. Methanol technology developments for the new millennium. *Appl. Catal. A-Gen.* **2001**, *221*, 275–282. [CrossRef]
3. Cantero, C.A.T.; Zuniga, R.P.; Garcia, M.M.; Cabral, S.R.; Calixto-Rodriguez, M.; Martinez, J.S.V.; Enriquez, M.G.M.; Estrada, A.J.P.; Torres, G.O.; Vazquez, F.D.S.; et al. Design and control applied to an extractive distillation column with salt for the production of bioethanol. *Processes* **2022**, *10*, 1792. [CrossRef]
4. Guzman-Martinez, C.E.; Maya-Yescas, R.; Castro-Montoya, A.J.; Rivera, F.N. Dynamic simulation of control systems for bioethanol reactive dehydration: Conventional and intensified case studies. *Chem. Eng. Process.* **2021**, *159*, 108238. [CrossRef]
5. Cantero, C.A.T.; Lopez, G.L.; Alvarado, V.M.; Jimenez, R.F.E.; Morales, J.Y.R.; Coronado, E.M.S. Control structures evaluation for a salt extractive distillation pilot plant: Application to bio-ethanol dehydration. *Energies* **2017**, *10*, 1276. [CrossRef]
6. De Figueiredo, M.F.; Brito, K.D.; Ramos, W.B.; Vasconcelos, L.G.S.; Brito, R.P. Effect of solvent content on the separation and the energy consumption of extractive distillation columns. *Chem. Eng. Commun.* **2015**, *202*, 1191–1199. [CrossRef]
7. Yin, C.F.; Liu, G.L. Optimization of solvent and extractive distillation sequence considering its integration with reactor. *Processes* **2021**, *9*, 565. [CrossRef]
8. Xue, X.C.; Gu, Q.F.; Pascal, H.; Darwesh, O.M.; Zhang, B.; Li, Z.Q. Simulation and optimization of three-column triple-effect methanol distillation scheme. *Chem. Eng. Process.* **2020**, *159*, 108229. [CrossRef]
9. Errico, M.; Pirellas, P.; Torres-Ortega, C.E.; Rong, B.G.; Segovia-Hernandez, J.G. A combined method for the design and optimization of intensified distillation systems. *Chem. Eng. Process.* **2014**, *85*, 69–76. [CrossRef]
10. Contreras-Zarazúa, G.; Vázquez-Castillo, J.A.; Ramírez-Márquez, C.; Segovia-Hernández, J.G.; Alcántara-Ávila, J.R. Multi-objective optimization involving cost and control properties in reactive distillation processes to produce diphenyl carbonate. *Comput. Chem. Eng.* **2016**, *105*, 185–196. [CrossRef]
11. Alcocer-García, H.; Segovia-Hernández, J.G.; Prado-Rubio, O.A.; Sánchez-Ramírez, E.; Quiroz-Ramírez, J.J. Multi-objective optimization of intensified processes for the purification of levulinic acid involving economic and environmental objectives. *Chem. Eng. Process.* **2019**, *136*, 123–137. [CrossRef]
12. Tarafder, A.; Lee, B.; Ray, A.K.; Rangaiah, G.P. Multiobjective optimization of an industrial ethylene reactor using a nondominated sorting genetic algorithm. *Ind. Eng. Chem. Res.* **2005**, *44*, 124–141. [CrossRef]
13. Mariano, A.P.; Borba Costa, C.B.; de Angelis, D.d.F.; Maugeri Filho, F.; Pires Atala, D.I.; Wolf Maciel, M.R.; Maciel Filho, R. Optimization of a fermentation process for butanol production by particle swarm optimization (PSO). *J. Chem. Technol. Biot.* **2010**, *85*, 934–949. [CrossRef]
14. Deb, K.; Jain, H. An evolutionary many-objective optimization algorithm using reference-point-based nondominated sorting approach, part I: Solving problems with box constraints. *IEEE Trans. Evol. Comput.* **2014**, *18*, 577–601. [CrossRef]
15. Pan, J.C.; Ding, J.H.; Zhang, C.D.; Wan, H.; Guan, G.F. Optimization and control for separation of ethyl benzene from C_8 aromatic hydrocarbons with extractive distillation. *Processes* **2022**, *10*, 2237. [CrossRef]
16. Hou, Y.; Wu, N.Q.; Li, Z.W.; Zhang, Y.X.; Qu, T.; Zhu, Q.H. Many-objective optimization for scheduling of crude oil operations based on NSGA-III with consideration of energy efficiency. *Swarm Evol. Comput.* **2020**, *57*, 100714. [CrossRef]

17. Brambilla, A.; Vaccari, M.; Pannocchia, G. Analytical RTO for a critical distillation process based on offline rigorous simulation. *IFAC-Pap.* **2022**, *55*, 143–148. [CrossRef]
18. Vaccari, M.; Pannocchia, G.; Tognotti, L.; Paci, M. Rigorous simulation of geothermal power plants to evaluate environmental performance of alternative configurations. *Renew. Energy* **2023**, *207*, 471–483. [CrossRef]
19. Hu, Z.H.; Li, P.L.; Liu, Y.F. Enhancing the performance of evolutionary algorithm by differential evolution for optimizing distillation sequence. *Molecules* **2022**, *27*, 3802. [CrossRef]
20. Su, Y.; Jin, S.M.; Zhang, X.P.; Shen, W.F.; Eden, M.R.; Ren, J.Z. Stakeholder-oriented multi-objective process optimization based on an improved genetic algorithm. *Comput. Chem. Eng.* **2019**, *132*, 106618. [CrossRef]
21. Douglas, J.M. *Conceptual Design of Chemical Processes*; McGraw-Hill, Inc.: New York, NY, USA, 1998.
22. Luyben, W.L. A counter-intuitive heuristic for specifying the composition of recycle streams. *Chem. Eng. Process.* **2018**, *133*, 234–244. [CrossRef]
23. Gadalla, M.A.; Olujic, Z.; Jansens, P.J.; Jobson, M.; Smith, R. Reducing CO_2 emissions and energy consumption of heat-integrated distillation systems. *Environ. Sci. Technol.* **2005**, *39*, 6860–6870. [CrossRef] [PubMed]
24. Czyzak, P.; Jaszkiewicz, A. Pareto simulated annealing-a metaheuristic technique for multiple-objective combinatorial optimization. *J. Multi-Crit. Decis. Anal.* **1998**, *7*, 34–47. [CrossRef]
25. Zitzler, E. Evolutionary Algorithms for Multiobjective Optimization: Methods and Applications. Ph.D. Thesis, Swiss Federal Institute of Technology, Zürich, Switzerland, 1999.
26. Yoon, K.S.; Hwang, C.L. Manufacturing plant location analysis by multiple attribute decision making: Part I—Single-plant strategy. *Int. J. Prod. Res.* **1985**, *23*, 345–359. [CrossRef]